Chemical Science

ROYAL SOCIETY OF CHEMISTRY

EDGE ARTICLE

View Article Online
View Journal | View Issue

Check for updates

Cite this: *Chem. Sci.*, 2024, **15**, 1409

All publication charges for this article have been paid for by the Royal Society of Chemistry

Open Access Article. Published on 07 December 2023. Downloaded on 2/7/2026 10:15:02 PM. This article is licensed under a Creative Commons Attribution-NonCommercial 3.0 Unported Licence.

Two active species from a single metal halide precursor: a case study of highly productive Mn-catalyzed dehydrogenation of amine-boranes *via* intermolecular bimetallic cooperation†

Ekaterina S. Gulyaeva,[ab] Elena S. Osipova,[b] Sergey A. Kovalenko,[b] Oleg A. Filippov, *[b] Natalia V. Belkova, [b] Laure Vendier,[a] Yves Canac, *[a] Elena S. Shubina *[b] and Dmitry A. Valyaev *[a]

Metal–metal cooperation for inert bond activation is a ubiquitous concept in coordination chemistry and catalysis. While the great majority of such transformations proceed *via* intramolecular mode in binuclear complexes, to date only a few examples of intermolecular small molecule activation using usually bimetallic frustrated Lewis pairs ($M^{\delta+}\cdots M'^{\delta-}$) have been reported. We introduce herein an alternative approach for the intermolecular bimetallic cooperativity observed in the catalytic dehydrogenation of amine-boranes, in which the concomitant activation of N–H and B–H bonds of the substrate *via* the synergetic action of Lewis acidic (M^{+}) and basic hydride (M–H) metal species derived from the same mononuclear complex (M–Br). It was also demonstrated that this system generated *in situ* from the air-stable Mn(I) complex *fac*-[(CO)$_3$(bis(NHC))MnBr] and $NaBPh_4$ shows high activity for H_2 production from several substrates (Me_2NHBH_3, *t*$BuNH_2BH_3$, $MeNH_2BH_3$, NH_3BH_3) at low catalyst loading (0.1% to 50 ppm), providing outstanding efficiency for Me_2NHBH_3 (TON up to 18 200) that is largely superior to all known 3d-, s-, p-, f-block metal derivatives and frustrated Lewis pairs (FLPs). These results represent a step forward towards more extensive use of intermolecular bimetallic cooperation concepts in modern homogeneous catalysis.

Received 9th October 2023
Accepted 6th December 2023

DOI: 10.1039/d3sc05356c

rsc.li/chemical-science

Introduction

Cooperative action of two metal atoms for the activation of organic molecules often accompanied by inert bond cleavage is omnipresent in heterogeneous catalysts,[1] metalloenzymes[2] and related biomimetic systems.[3] In coordination chemistry, these processes generally take place intramolecularly within well-defined homo- or heterobimetallic complexes (Scheme 1(a)), in which two metal atoms are kept in close proximity by bridging ligand(s)[3] occasionally supported by additional metal–metal interaction.[4] Similar reactivity has also been observed for binuclear derivatives with a highly polarized metal–metal single bond (Scheme 1(b)), also known as metal-only Lewis pairs (MOLPs).[5,6] In the latter case, if the inert bond of the substrate is completely cleaved, the two resulting monometallic species can participate in a single catalytic cycle with a synergetic effect.[7] In sharp contrast, the intermolecular cooperative activation of small molecules mediated by two mononuclear transition metal species (Scheme 1(c)) remains rare.[8] The most pertinent examples of such behavior deal with the interaction of bimetallic frustrated Lewis pairs (FLPs) with dihydrogen,[9] acetylene,[9c] amine-boranes[10] or formic acid.[11] Conceptually related intermolecular activation of CO_2 and epoxide by a radical pair arising from the spontaneous homolytic cleavage of a Fe–Al bond in a bimetallic complex prior to interaction with a substrate was also recently reported.[12] Despite remarkable results already achieved in the area of homogeneous catalysis exploiting bimetallic cooperation, in most cases either quite sophisticated binuclear transition metal complexes (Scheme 1(a and b))[3–7] or a carefully selected combination of two monometallic species (Scheme 1(c))[10] were employed. In this contribution, we provide experimental and theoretical evidence for a novel type of intermolecular bimetallic cooperativity using Lewis acidic and hydride components (Scheme 1(d)) generated *in situ* from a single mononuclear metal precursor, halide abstractor and

[a]*LCC-CNRS, Université de Toulouse, CNRS, UPS, 205 Route de Narbonne, 31077 Toulouse Cedex 4, France. E-mail: yves.canac@lcc-toulouse.fr; dmitry.valyaev@lcc-toulouse.fr*

[b]*A. N. Nesmeyanov Institute of Organoelement Compounds (INEOS), Russian Academy of Sciences, 28/1 Vavilov Str., GSP-1, B-334, Moscow, 119334, Russia. E-mail: h-bond@ineos.ac.ru; shu@ineos.ac.ru*

† Electronic supplementary information (ESI) available: Complete experimental procedures, details of DFT calculations, original IR and NMR spectra and kinetic profiles for H_2 evolution. CCDC 2262301 and 2262302. For ESI and crystallographic data in CIF or other electronic format see DOI: https://doi.org/10.1039/d3sc05356c

© 2024 The Author(s). Published by the Royal Society of Chemistry

Open Access Article. Published on 07 December 2023. Downloaded on 2/7/2026 10:15:02 PM. This article is licensed under a Creative Commons Attribution-NonCommercial 3.0 Unported Licence.

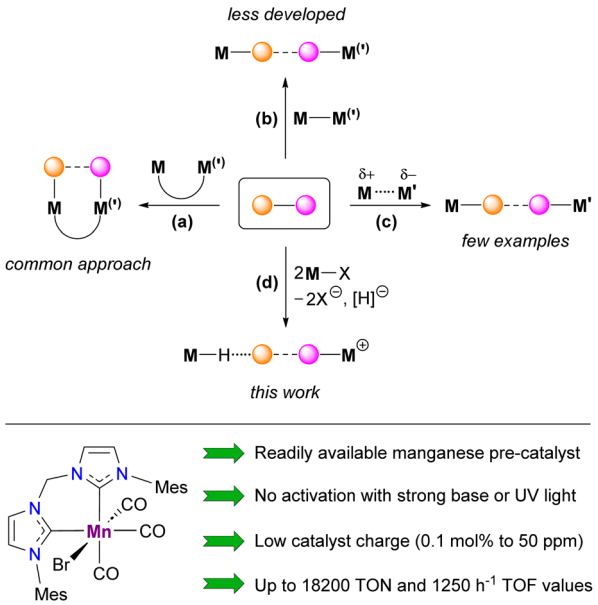

Scheme 1 Different types of cooperative bimetallic activation of organic molecules (top, dashed and dotted lines refer to activated/cleaved bonds in the substrate and non-covalent interactions, respectively) and the Mn(I) precursor used for catalytic intermolecular amine-borane dehydrogenation (bottom).

bifunctional substrate. Beyond the apparent simplicity of this approach, its potential usefulness was illustrated by the development of a convenient procedure for dehydrogenation of various amine-boranes catalyzed by an air-stable Mn(I) bis(NHC) complex (Scheme 1, bottom), showing, in particular, state-of-the-art performance for H_2 production from Me_2NHBH_3 (DMAB) that largely surpasses those of all known 3d metal catalysts.

Results and discussion

Discovery and optimization of amine-borane dehydrogenation catalyzed by Mn(I) *fac*-[(CO)$_3$(L–L′)MnBr] (L, L′ = phosphine, NHC) complexes

In the frame of our research dealing with Mn(I) organometallic chemistry relevant to homogeneous catalysis, we have unexpectedly observed that the cationic complex $[\mathbf{1}^{\mathbf{BuCl}}]^+$ (Scheme 2)[13] obtained by reaction of the corresponding hydride $\mathbf{1}^{\mathbf{H}}$ with $[Ph_3C](B(C_6F_5)_4)$ in *n*BuCl is capable of catalyzing DMAB dehydrogenation at 50 °C to produce H_2 with a turnover frequency (TOF) of *ca.* 0.6 h^{-1}. Further studies have revealed that parent cationic species $[\mathbf{2}^{\mathbf{BuCl}}]^+$ and $[\mathbf{3}^{\mathbf{BuCl}}]^+$,[14] in which Ph_2P moieties are progressively replaced with more donating N-heterocyclic carbene (NHC) fragments, are much more active, affording TOFs of 9 h^{-1} and 143 h^{-1}, respectively. Encouraged by the latter result being more superior to the performance of previously known Mn-based catalysts for this substrate (TOF 0.7–11 h^{-1}),[15] we proceeded to further optimization of this catalytic system.

Looking for a more convenient source of cationic Mn(I) species, we first prepared the corresponding MeCN complex $[\mathbf{3}^{\mathbf{MeCN}}](BF_4)$ from $AgBF_4$ and the readily available bromide precursor $\mathbf{3}^{\mathbf{Br}}$.[16] This compound was isolated in 85% yield and fully characterized, including single-crystal X-ray diffraction (Fig. S1†). While this compound showed very low activity in *n*BuCl, the use of a more chemically inert chlorinated solvent such as PhCl allowed almost quantitative DMAB conversion at only 0.1 mol% catalyst charge (Table 1, entry 1). Gratifyingly, the catalyst can also be generated *in situ* from $\mathbf{3}^{\mathbf{Br}}$ and $NaBF_4$ (Table 1, entry 2) even if its activity is lower than that of the isolated $[\mathbf{3}^{\mathbf{MeCN}}](BF_4)$ complex. The application of sodium salts with non-coordinating anions boosted the catalyst performance (Table 1, entries 3 and 4) being better than for the initially tested complex $[\mathbf{3}^{\mathbf{BuCl}}]^+$ in *n*BuCl (*vide supra*). Solvent screening revealed that PhF provided slightly inferior results (Table 1, entry 5), whereas the use of coordinating THF led to a serious drop in the reaction rate (Table 1, entry 6). The reaction even slowly proceeds in dichloromethane at 30 °C (Table 1, entry 7), albeit with a ten-fold higher catalyst loading. The addition of mercury did not alter the dehydrogenation process (Table 1, entry 8), thus ruling out the well-known catalysis of amine-borane dehydrogenation

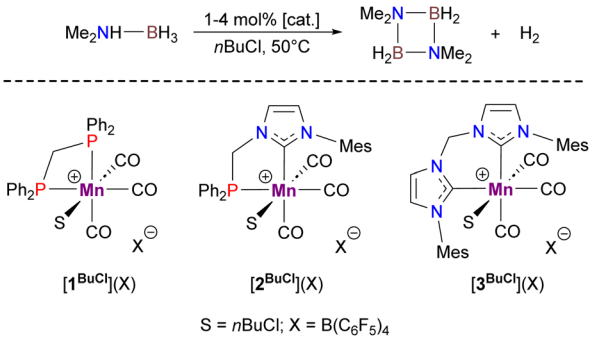

Scheme 2 DMAB dehydrogenation catalyzed by cationic Mn(I) complexes $[\mathbf{1}–\mathbf{3}^{\mathbf{BuCl}}](B(C_6F_5)_4)$.

Table 1 Optimization of DMAB dehydrogenation catalyzed by bis(NHC) Mn(I) complexes[a]

No.	Pre-catalyst	Solv.	Additive	Time, h	TON[b]	TOF[c], h^{-1}
1	$[\mathbf{3}^{\mathbf{MeCN}}](BF_4)$	PhCl	—	26	981	38
2	$\mathbf{3}^{\mathbf{Br}}$	PhCl	$NaBF_4$	69	902	13
3	$\mathbf{3}^{\mathbf{Br}}$	PhCl	$NaBPh_4$	3.9	1000	259
4	$\mathbf{3}^{\mathbf{Br}}$	PhCl	$NaB(C_6F_5)_4$	4.1	1000	244
5	$\mathbf{3}^{\mathbf{Br}}$	PhF	$NaBPh_4$	6.7	1000	149
6	$\mathbf{3}^{\mathbf{Br}}$	THF	$NaBPh_4$	26	1000	38
7[d]	$\mathbf{3}^{\mathbf{Br}}$	DCM	$NaBPh_4$	11	100	9
8[e]	$\mathbf{3}^{\mathbf{Br}}$	PhCl	$NaBPh_4$	4.0	1000	256
9	$\mathbf{3}^{\mathbf{Br}}$	PhCl	—	118	535	5
10	$\mathbf{3}^{\mathbf{H}}$	PhCl	—	69	253	4

[a] DMAB (1.5 mmol), 0.1 mol% of pre-catalyst, 1.0 mol% of sodium salt, 2 mL of solvent in a closed vessel at 50 °C. [b] Estimated from the pressure changes due to H_2 release under constant volume conditions. [c] TOF values were calculated based on a 10–20 min induction period required for catalyst activation. [d] 1 mol% of $\mathbf{3}^{\mathbf{Br}}$ and 10 mol% of $NaBPh_4$ at 30 °C. [e] Reaction in the presence of 250 equivalents of mercury.

© 2024 The Author(s). Published by the Royal Society of Chemistry

Open Access Article. Published on 07 December 2023. Downloaded on 2/7/2026 10:15:02 PM. This article is licensed under a Creative Commons Attribution-NonCommercial 3.0 Unported Licence.

by metal nanoparticles.[17,18] Finally, it was observed that neutral $\mathbf{3^{Br}}$ and $\mathbf{3^{H}}$ without any additives displayed only modest catalytic activity (Table 1, entries 9 and 10).

Then, we focused on the evaluation of the catalytic performance of this system (Table 2). At 60 °C, the reaction rate is significantly accelerated (Table 2, entry 1) and the catalyst charge may be decreased to 50 ppm, resulting in turnover number (TON) and turnover frequencies (TOF) values of 16 221, and 661 h^{-1}, respectively (Table 2, entries 2–4). Surprisingly, we noted that the reaction was even faster in the dark, providing a TON of 18 242 at a 50 ppm charge for $\mathbf{3^{Br}}$ (Table 2, entry 5), probably preventing photo-induced catalyst decomposition. Background DMAB dehydrogenation in the presence of $NaBPh_4$ under these conditions was not observed at all (Table 2, entry 6). Remarkably, the catalytic performance of this substrate is more than 50 times higher than those previously observed for 3d metal catalysts (20–330 TONs),[15,19] especially considering that activation by strong bases (*n*BuLi, *t*BuOK)[19a,e,f] or UV-light[15b,c,19c,g] was required for most of these systems. The results obtained for catalyst $\mathbf{3^{Br}}$ also surpass significantly the TON values obtained for noble metal derivatives (up to a TON of 2240),[20] s-, p- and f-block metal complexes (up to a TON of 485)[21–25] as well as FLP-based systems (up to a TON of 500).[26] The only comparable precedent in terms of productivity was reported for $Ru(acac)_3$/oleylamine combination (TON = 15 000),[27] however, the reaction rate in this case was much slower (TOF 78 h^{-1} at 60 °C).

We found that our system is also suitable for amine-boranes with a higher hydrogen content relevant for hydrogen storage materials.[28] Preliminary results without any additional optimization showed that tBuNH$_2$BH$_3$ can release *ca.* 1.53 equivalents of H_2 with a catalyst charge of only 0.1 mol% (Table 2, entry 7). Though this substrate can be slowly dehydrogenated under these conditions without any catalyst (Table 2, entry 8), the Mn-catalyzed reaction was much faster, producing *ca.* 1.3 equivalents of hydrogen after 10 h (TOF of 130 h^{-1} for this period) followed by a more sluggish process releasing a further 0.2 equivalents in *ca.* 40 h (Fig. S13†). To the best of our knowledge, this value represents the best result ever obtained for this substrate among all other metal complexes.[10,23b,25a,29] ^{11}B NMR analysis of the crude reaction mixture (Fig. S15†) revealed the presence of substituted borazine $[t\text{BuNBH}]_3$, cyclic trimer $[t\text{BuNHBH}_2]_3$ and oligomers $[t\text{Bu}_3\text{NHBH}_2]_n$ as the main dehydrogenation products. We supposed that the drop in the reaction rate after evolution of the first equivalent of hydrogen was due to the more difficult uptake of partially dehydrogenated products by our catalytic system. Dehydrogenation of MeNH$_2$-BH$_3$ (Table 2, entry 9) was found to be slightly slower than in the case of tBuNH$_2$BH$_3$ (TOF of 123 h^{-1} for a 10 h period) and less efficient in terms of the amount of produced H_2 (1.2 equivalents, Fig. S13†), probably due to the lower solubility of this substrate in PhCl and the extensive formation of insoluble polymeric products $[\text{MeNHBH}_2]_n$. However, the catalytic efficiency attained in this case (TON of 1343) is competitive compared to the majority of known 3d metal catalysts (TONs of 20–250)[30] and remains inferior only to highly active Co-based complexes (TONs of up to 5000).[31] Finally, the reaction of NH_3BH_3 afforded 0.61 equivalents of H_2 in 60 h (Table 2, entry 11) leading to the formation of an insoluble polymer $[\text{NH}_2\text{BH}_2]_n$. The TON value was estimated to be in the range of 500–550 considering the background substrate dehydrogenation process (Table 2, entry 12). However, despite slow reaction kinetics and a low amount of produced dihydrogen compared to the best catalytic systems based on first row transition metal complexes[32] or purely organic molecules[33] working at 1–5 mol% catalyst charge (1.7–2.5 equiv. of H_2 per NH_3BH_3), these numbers are still superior in terms of overall performance to previously reported Mn-based catalysts (TON *ca.* 50–70).[34] Considering the remarkable progress recently achieved in formic acid dehydrogenation using Mn(I) complexes,[35] our results further highlight the privileged position of this metal in the future design of sustainable homogeneous catalysts for H_2 production.

Table 2 Dehydrogenation of various amine-boranes catalyzed by bis(NHC) Mn(I) complex $\mathbf{3^{Br}}$[a]

No.	Substrate	$\mathbf{3^{Br}}$, mol%	Time, h	H_2, eq.[b,c]	TON (TOF, h^{-1})[b,c]
1	DMAB	0.1	2.1	>0.99	1000 (476)
2	DMAB	0.02	4.8	>0.99	5000 (1058)
3	DMAB	0.01	8.7	>0.99	10 000 (1157)
4	DMAB	0.005	24.6	0.81	16 221 (661)
5	DMAB	0.005[d]	14.4	0.91	18 242 (1267)
6	DMAB	—	60	<0.01[e]	—
7	tBuNH$_2$BH$_3$	0.1[d]	48.6	1.53	1527 (31)
8	tBuNH$_2$BH$_3$	—	60	0.36[e]	—
9	MeNH$_2$BH$_3$	0.1[d]	28.4	1.34	1343 (47)
10	MeNH$_2$BH$_3$	—	60	0.2[e]	—
11	NH_3BH_3	0.1[d]	60	0.61	611 (10)
12	NH_3BH_3	—	60	0.07[e]	—

[a] Amine-borane (0.8–1.5 mmol), 0.5–1.0 mol% of $NaBPh_4$, 2 mL of PhCl in a sealed vessel at 60 °C. [b] Average from two independent runs. [c] Estimated from the pressure changes due to H_2 release under constant volume conditions and ^{11}B NMR spectra of the crude products. [d] In the dark. [e] Background dehydrogenation experiments were carried out in the presence of 1.0 mol% of $NaBPh_4$ under strictly identical conditions to those of the Mn-catalyzed process.

Spectroscopic and kinetic studies of the reaction mechanism for DMAB dehydrogenation catalyzed by the Mn(I) complex *fac*-[(CO)$_3$(bis(NHC))MnBr] ($\mathbf{3^{Br}}$)

Next, we turned our attention to a deeper understanding of this catalytic system, as all conventional known mechanisms for transition metal-catalyzed amine-borane dehydrogenation[36] based on either metal–ligand cooperation (Scheme 3(a)), reactivity of coordinatively unsaturated hydrides (Scheme 3(b)) or bimetallic activation (Scheme 3(c)) are *a priori* inappropriate in this case. Firstly, regarding possible metal–ligand cooperation, it should be noted that the non-innocent character of dppm[37] and NHC-phosphine[38] ligands due to the deprotonation of the CH_2 bridge in the corresponding Mn(I) bromide complexes may only be observed in the presence of strong base, which is not required in the present case. Furthermore, no evidence for the cooperative behavior of the bis(NHC) ligand incorporated into the most active catalyst has been reported so far, which thus

Open Access Article. Published on 07 December 2023. Downloaded on 2/7/2026 10:15:02 PM. This article is licensed under a Creative Commons Attribution-NonCommercial 3.0 Unported Licence.

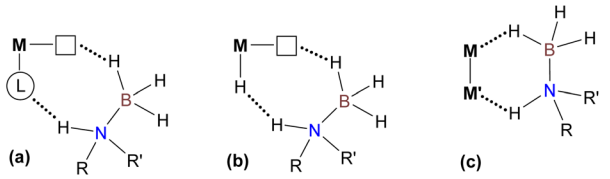

Scheme 3 An overview of the main known approaches for amine-borane dehydrogenation catalyzed by transition metal complexes.

permitted us to exclude path (a). Then, despite extensive applications of different manganese bis(NHC) complexes in hydrosilylation,[16a,39] electrochemical CO_2 reduction,[16b,40] hydrogenation[41] and hydrogen-borrowing processes[42] systematically involving hydride *fac*-[$(CO)_3$(bis(NHC))MnH] intermediates, the dissociation of a CO ligand in such species has never been proved experimentally. Moreover, the formation of the dicarbonyl complex *fac*-[$(CO)_2(\eta^2\text{-}H_2)$(bis(NHC))MnH] from H_2 and a tricarbonyl hydride precursor was recently proposed in a Mn-catalyzed ester hydrogenation mechanism,[42a] but the calculated barrier for the CO-to-H_2 substitution of 38.5 kcal mol^{-1} seems too high for our reaction conditions, thus making path (b) very unlikely (*vide infra*). Finally, the bimetallic activation pathway[43] (Scheme 3(c)) can also be ruled out because of the insufficient reducing ability of amine-boranes to form Mn(0) derivatives from $\mathbf{3^{Br}}$ and the apparent impossibility of metal–metal bond formation to generate a [$(CO)_3$(bis(NHC))Mn] radical due to steric hindrance.[40b]

We started our mechanistic investigations from the operando spectroscopic monitoring of the catalytic process in CH_2Cl_2. This solvent was chosen instead of PhCl because of slower reaction kinetics (Table 1), its full transparency in ν_{CO} region and the availability of its deuterated version for NMR studies. Similar trends were also observed in PhCl (Fig. S19†) albeit that a full set of spectroscopic data for reaction intermediates cannot be obtained in this solvent (see the ESI† for details). The analysis of the IR spectra of $\mathbf{3^{Br}}$/$NaBPh_4$/DMAB solution in the ν_{CO} region (Fig. 1) revealed an initial transformation of the starting bromide into the cationic species [$\mathbf{3^{DMAB}}$](BPh_4) with a coordinated substrate (Fig. 1(a)). Subsequent evolution of the latter into the hydride $\mathbf{3^{H}}$ (Fig. 1(b)) is consistent with the induction period observed by volumetric H_2 evolution studies (*vide infra*). The concomitant conversion of DMAB into the dimer $[Me_2NBH_2]_2$ was evident from characteristic changes in the ν_{BH} region (Fig. S18†). After full DMAB consumption, $\mathbf{3^{H}}$ rapidly decayed to give a mixture of neutral chloride compound $\mathbf{3^{Cl}}$ and the cationic complex [$\mathbf{3^{(Me_2NBH_2)_2}}$]($BPh_4$) bearing a coordinated $[Me_2NBH_2]_2$ ligand (Fig. 1(c), see Fig. S17† for ν_{CO} band deconvolution). ^{11}B NMR monitoring of the reaction mixture in CD_2Cl_2 (Fig. S23†) showed the appearance of the characteristic signal of $Me_2N{=}BH_2$ at δ_B 37.4 ppm, consistent with an "off-metal" dimerization mechanism for the formation of the final product.[36] The ^1H NMR spectra (Fig. S21†) confirmed the presence of the hydride complex $\mathbf{3^{H}}$ at δ_H −7.04 ppm and additionally revealed a broad signal at δ_H −3.38 ppm. We were able to retrieve a full set of NMR data for this intermediate (see the ESI†), attributed to a cationic Mn(I) σ-borane complex [$\mathbf{3^{DMAB}}$](BPh_4).

In order to confirm this assignment, we prepared the model Mn(I) cationic complex [$\mathbf{3^{Me_3NBH_3}}$](BPh_4) from Me_3NBH_3 that is unreactive towards dehydrogenation, $\mathbf{3^{Br}}$ and $NaBPh_4$. Its structure elucidated from X-ray diffraction measurements (Fig. 2) features a η^1-BH coordination mode previously observed in half-sandwich Mn(I) analogues.[44] The BH_3 moiety in the NMR spectra of [$\mathbf{3^{Me_3NBH_3}}$](BPh_4) appears as broad signals at δ_B −11.9 ppm and δ_H −3.30 ppm. The latter value matches well with that observed during the NMR mechanistic investigation, clearly indicating the participation of such species in the catalytic process. According to IR and NMR data, all transformations occurring in catalytic DMAB dehydrogenation involved only tricarbonyl Mn(I) complexes and we did not find any spectroscopic evidence for the formation of the neutral dicarbonyl hydride species *fac*-[$(CO)_2$(DMAB)(bis(NHC))MnH] essential for the realization of the route (b), as depicted in Scheme 3.

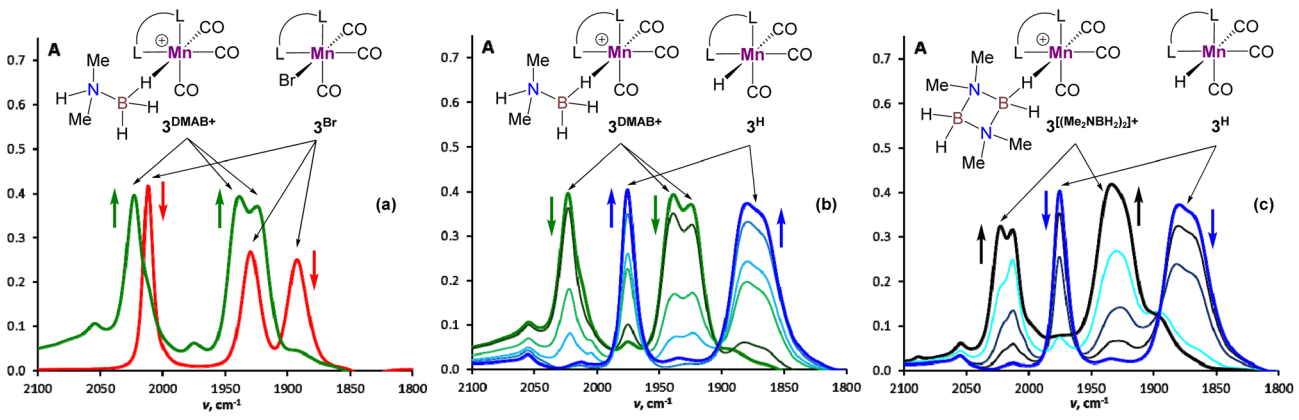

Fig. 1 IR spectroscopy monitoring in the ν_{CO} range for DMAB dehydrogenation in the presence of $\mathbf{3^{Br}}$ (3.3 mol%) and $NaBPh_4$ (16.5 mol%) in CH_2Cl_2 at *ca.* 30 °C (L–L = bis(NHC), *c*(DMAB) = 0.30 M, *l* = 0.01 cm). (a) IR spectra of the initial $\mathbf{3^{Br}}$ solution (red) and reaction mixture after 2 min upon DMAB addition (green). (b) IR spectra between 2 min (green) and 20 min (blue) of reaction time. (c) IR spectra between 20 min (blue) and 40 min (black) of reaction time.

© 2024 The Author(s). Published by the Royal Society of Chemistry

Open Access Article. Published on 07 December 2023. Downloaded on 2/7/2026 10:15:02 PM.
This article is licensed under a Creative Commons Attribution-NonCommercial 3.0 Unported Licence.

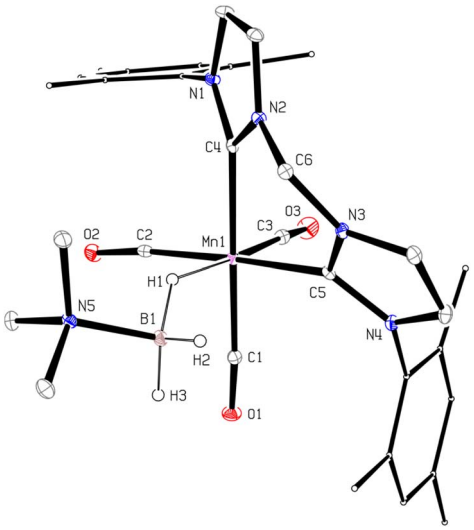

Fig. 2 Molecular geometry of the complex $[\mathbf{3}^{\mathbf{Me_3NBH_3}}](BPh_4)$ (20% probability ellipsoids, Mes groups represented as a wireframe, most hydrogen atoms, BPh_4^- anion and CH_2Cl_2 solvate molecules are not shown).

The kinetic studies revealed [pseudo]zero order for the substrate (Fig. S27†) and first order for catalyst concentration (Fig. S28†). The variation in the amount of $NaBPh_4$ (0.125–8 mol%) showed virtually no influence on the reaction rate (Fig. S29†), thus ruling out the occurrence of a conceptually similar DMAB dehydrogenation process that proceeds *via* a Na^+/Mn–H couple. While the reversible coordination of a sodium cation with DMAB cannot be excluded, we supposed that this interaction is too weak to activate the substrate towards deprotonation with the Mn(I) hydride complex $\mathbf{3}^{\mathbf{H}}$ (*vide infra*). Variable-temperature experiments in the 30–60 °C range (Fig. 3) allowed estimation of the activation enthalpy $\Delta H^{\ddagger} = 14.5 \pm 0.4$ kcal mol^{-1} (Fig. S26 and Table S6†), which is typical for proton transfer to transition metal hydrides.[45] The detailed description of the proposed kinetic model is provided in the ESI.† Finally, kinetic isotope effects (k_H/k_D, Fig. 4) measured at 60 °C for Me_2NHBD_3 (1.5 ± 0.1), Me_2NDBH_3 (2.1 ± 0.1) and Me_2NDBD_3 (2.9 ± 0.1) are consistent with the involvement of B–H and N–H bond cleavage in the rate determining step.[32a,c] These data taken together with spectroscopic results show the implication of cationic and hydride Mn(I) species in the catalytic process, allowing us to propose an unconventional intermolecular DMAB activation, which was then studied by theoretical means.

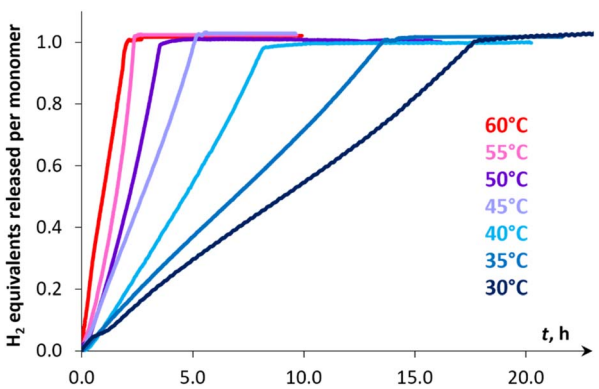

Fig. 3 Hydrogen evolution kinetic curves of DMAB dehydrogenation in PhCl catalyzed by $\mathbf{3}^{\mathbf{Br}}$ (0.1 mol%) and $NaBPh_4$ (1 mol%) at various temperatures. The initial parts of the curves corresponding to the induction period (10–20 min) are not shown.

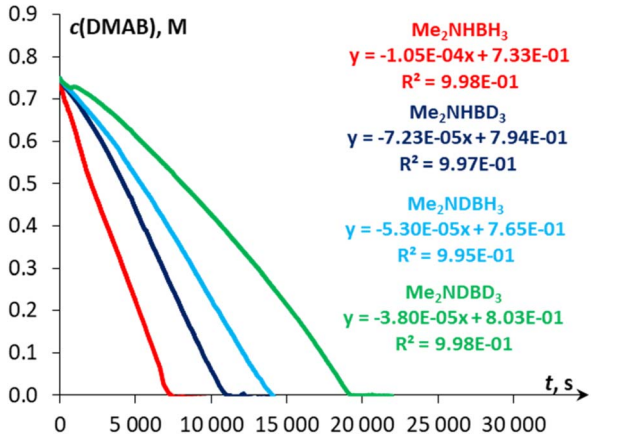

Fig. 4 *c*(DMAB) *vs.* time plots for the initial reaction rate determination of Me_2NHBH_3, Me_2NHBD_3, Me_2NDBH_3 and Me_2NDBD_3 ($c_0 = 0.75$ M) dehydrogenation catalyzed by $\mathbf{3}^{\mathbf{Br}}$ (0.1 mol%) in the presence of $NaBPh_4$ (1.0 mol%) in PhCl at 60 °C.

Theoretical investigation of DMAB dehydrogenation catalyzed by the Mn(I) complex *fac*-[(CO)$_3$(bis(NHC))MnBr] ($\mathbf{3}^{\mathbf{Br}}$)

Computational modelling of the catalytic system showed that the monometallic species $\mathbf{3}^+$ and $\mathbf{3}^{\mathbf{H}}$ interact with DMAB (Fig. 5) *via* B–H coordination and dihydrogen bonding, respectively. However, activation barriers for the subsequent hydride and proton transfer steps in these intermediates $[\mathbf{3}^{\mathbf{DMAB}}]^+$ and $\mathbf{3}^{\mathbf{H}}\cdots$DMAB exceed 30–40 kcal mol^{-1} and no stabilization of the resulting products was observed from DFT calculations (Fig. S31 and S33†). In contrast, proton transfer becomes feasible in the most thermodynamically stable adduct $\mathbf{4}^+$, in which two metal fragments are bridged by a DMAB molecule. Both the N–H (1.040 Å) and B–H (1.264 Å) bonds of the coordinated DMAB moiety in $\mathbf{4}^+$ are slightly longer than those in the corresponding mononuclear species $\mathbf{3}^{\mathbf{H}}\cdots$DMAB (1.028 Å) and $\mathbf{3}^{\mathbf{DMAB+}}$ (1.258 Å) thus being consistent with a greater extent of substrate activation. This process leads initially to the formation of bimetallic intermediate $\mathbf{5}\cdots\mathbf{3}^{\mathbf{H_2}+}$, which is composed of the cationic dihydrogen complex $[\mathbf{3}^{\mathbf{H_2}}]^+$ associated with the zwitter-ionic species **5** by hydrogen bonding (2.283 Å), then undergoing dissociation to the individual components. Importantly, the metal-coordinated B–H bond distance in complexes $\mathbf{5}\cdots\mathbf{3}^{\mathbf{H_2}+}$ and **5** becomes elongated by 0.093 and 0.234 Å, respectively, relative to that in $\mathbf{4}^+$ with a concomitant shortening of the Mn–H distance by 0.056 and 0.109 Å, respectively. These data are in agreement with the occurrence of a progressive hydride transfer in the sequence of $\mathbf{5}\cdots\mathbf{3}^{\mathbf{H_2}+} \rightarrow \mathbf{5} \rightarrow \mathbf{3}^{\mathbf{H}}\cdots BH_2{=}NMe_2$. Finally, the essentially barrierless loss of H_2 and $Me_2N{=}BH_2$ from $[\mathbf{3}^{\mathbf{H_2}}]^+$ and

Open Access Article. Published on 07 December 2023. Downloaded on 2/7/2026 10:15:02 PM. This article is licensed under a Creative Commons Attribution-NonCommercial 3.0 Unported Licence.

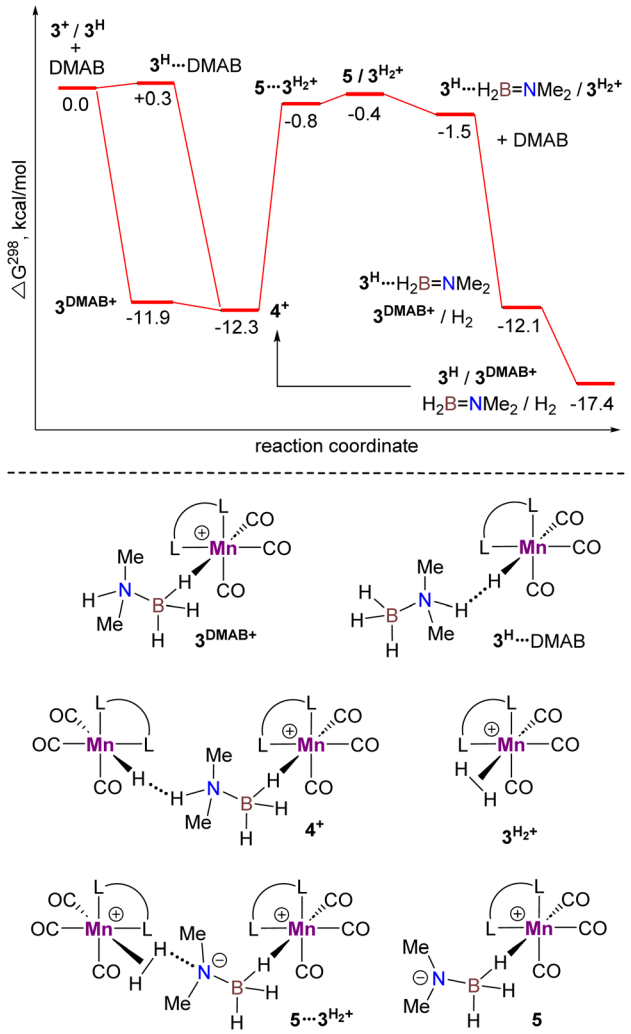

Fig. 5 Calculated Gibbs energy profile for DMAB dehydrogenation catalyzed by a $3^{+}/3^{H}$ couple at the ωB97XD/def2-TZVP level in toluene (dihydrogen bond interactions are indicated as dotted lines, non-interacting molecules are separated by a slash) and structures of the key intermediates (bottom).

$3^{H}\cdots BH_2{=}NMe_2$, respectively regenerate a $3^{+}/3^{H}$ couple, thus exhibiting a curious interconversion of both metal species after each catalytic turnover. The key role of the bimetallic adducts 4^{+} and $5\cdots3^{H_2+}$ in the DMAB activation process provides additional evidence to consider this reaction mechanism as a viable intermolecular bimetallic cooperation (Scheme 1(d)).

Proposed catalytic cycle for DMAB dehydrogenation catalyzed by the Mn(I) complex *fac*-[(CO)$_3$(bis(NHC))MnBr] (3^{Br})

The catalytic cycle for DMAB dehydrogenation emerging from the results of the spectroscopic and kinetic studies combined with the DFT calculations is shown in Scheme 4. The activation steps (Scheme 4, top) include bromide abstraction from 3^{Br} with $NaBPh_4$ in the presence of a substrate to afford the cationic intermediate [3^{DMAB}](BPh_4). Its slow deprotonation by traces of amine and/or water followed by hydride transfer presumably leads to the initial accumulation of 3^{H} essential for the catalytic process. Indeed, the addition of isolated 3^{H} to a 3^{Br}/$NaBPh_4$/DMAB mixture resulted in immediate H_2 evolution without any induction period (Fig. 6). Interestingly, the formation of a ternary adduct [**4**](BPh_4) is favorable in terms of Gibbs energy regardless of the large entropy effect. This intermediate undergoes a sequence of N–H/B–H bond cleavage steps, ultimately affording 3^{H}, $Me_2N{=}BH_2$, and [3^{H_2}](BPh_4), which rapidly exchanges the H_2 ligand for DMAB and thus restores the initial [3^{DMAB}](BPh_4). The first-order kinetics on the metal, spectroscopic detection of 3^{H} as a resting state and KIE values are consistent with the low steady-state concentration of the cation [3^{DMAB}](BPh_4) in the reaction mixture and its deprotonation by 3^{H} *via* the formation of [**4**](BPh_4) as the rate-determining step. Thus, the overall reaction rate is dependent on variable 3^{DMAB+} concentration, while 3^{H} concentration remains constant and gives the effective reaction rate law: $r_3 = k_{eff}[3^{DMAB+}]$ (see Scheme S2 and the associated text in the ESI† for a complete kinetic model). For this reason, despite the simultaneous presence of two metal complexes (3^{H} and 3^{DMAB+}) in the reaction mixture, first reaction order in overall metal concentration was actually observed. In this context, the beneficial effect of NHC on the series of Mn(I) complexes with bidentate ligands (Scheme 2) can be rationalized due to the synergy between a better stabilization of the cationic species and a higher basicity of the corresponding hydrides. Importantly, complex 3^{H} may be observed in the reaction mixture uniquely in the presence of an amine-borane substrate, whereas isolated hydride decomposes rapidly in PhCl at 50–60 °C to form mainly chloride derivative 3^{Cl}. We suppose that such counter-intuitive survival of 3^{H} in a variety of chlorinated solvents (*n*BuCl, PhCl, CH_2Cl_2) may be explained by the faster dehydrogenation kinetics *vs.* chlorination and efficient regeneration of the cationic complex [3^{DMAB}]$^{+}$ from 3^{Cl} by the

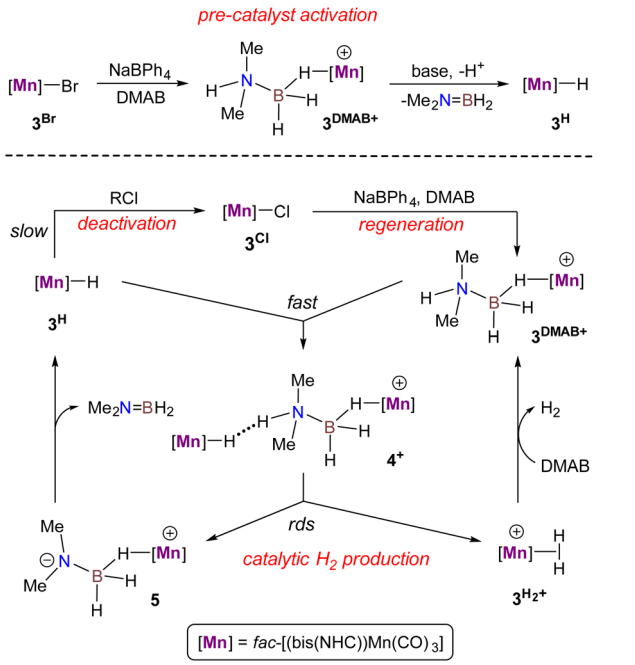

Scheme 4 Proposed mechanism for DMAB dehydrogenation catalyzed by the bis(NHC) Mn(I) complex 3^{Br}.

© 2024 The Author(s). Published by the Royal Society of Chemistry

Open Access Article. Published on 07 December 2023. Downloaded on 2/7/2026 10:15:02 PM.
This article is licensed under a Creative Commons Attribution-NonCommercial 3.0 Unported Licence.

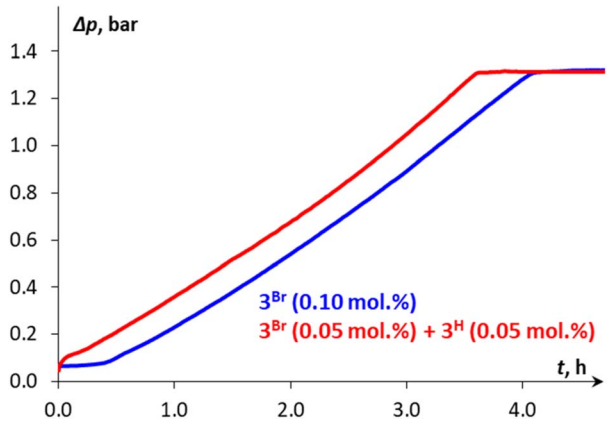

Fig. 6 Kinetic profile (Δ*p vs.* time) for DMAB dehydrogenation in PhCl at 50 °C catalyzed either by 0.1 mol% $\mathbf{3}^{Br}$ or by a mixture of $\mathbf{3}^{Br}$ (0.05 mol%) and $\mathbf{3}^{H}$ (0.05 mol%) in the presence of $NaBPh_4$ (1 mol%).

excess of halide abstractor (Scheme 4), thus explaining the observed trend in the catalytic activity in the order of PhCl ≫ *n*BuCl > CH_2Cl_2 and the overall robustness of our catalytic system that results in high TON values.

Conclusions

We have evidenced by spectroscopic, kinetic and theoretical means a new type of intermolecular bimetallic cooperativity between hydride and cationic species, clearly illustrating that a simple mononuclear metal halide precursor can be at the origin of two catalytically active species actually doing two complementary jobs for one price. The potential of this approach for homogeneous catalysis was demonstrated by the development of a practical and efficient system for amine-borane dehydrogenation based on an air-stable bis(NHC) Mn(I) complex and $NaBPh_4$ that is capable of operating at low catalyst charge and providing unprecedented TONs for Me_2NHBH_3 and *t*$BuNH_2BH_3$ substrates. Our results also show that nucleophilic metal hydrides can successfully operate in chlorinated solvents if the catalytic process is faster than decomposition, thus allowing us to shake up a longstanding paradigm about their incompatibility. Taking into account a plethora of known monometallic halide complexes bearing strong donor ligands, we hope that this contribution will boost the interest of a broader use of intermolecular bimetallic cooperation phenomena in organometallic chemistry and homogeneous catalysis.

Data availability

All relevant experimental data and details of the DFT calculations are provided in the ESI.† Deposition numbers 2262301 (for $[\mathbf{3}^{MeCN}](BF_4)$) and 2262302 (for $[\mathbf{3}^{Me_3NBH_3}](BPh_4)$) contain the supplementary crystallographic data for this paper.

Author contributions

O. A. F., N. V. B., E. S. S., Y. C. and D. A. V. planned and guided the research project. E. S. O. and D. A. V. acquired the research funding. E. S. G. carried out the main experimental work and performed initial data analysis. E. S. O. and S. A. K. participated in IR mechanistic investigations. O. A. F. performed the DFT calculations. L. V. and D. A. V. carried out X-ray diffraction experiments. E. S. G., E. S. O., O. A. F., N. V. B., E. S. S., Y. C. and D. A. V. participated in manuscript preparation. All authors have approved the final version of the manuscript.

Conflicts of interest

There are no conflicts to declare.

Acknowledgements

The work was financially supported by the Russian Science Foundation (grant no. 22-73-00072, spectroscopic mechanistic studies) and by the CNRS. E. S. G. is grateful to the French Embassy in Moscow for a joint PhD fellowship (Vernadski program). Computational studies were performed using HPC resources from CALMIP (grant no. P18038). Spectroscopic data were partially collected using the equipment of the Center for Molecular Composition Studies of INEOS RAS with the support from the Ministry of Science and Higher Education of the Russian Federation (contract no. 075-03-2023-642). We thank Dr Noël Lugan and Dr Olivier Baslé for helpful discussions.

References

1 (*a*) L. Liu and A. Corma, *Chem. Rev.*, 2023, **123**, 4855–4933; (*b*) L. Liu and A. Corma, *Chem. Rev.*, 2018, **118**, 4981–5079.
2 R. H. Holm, P. Kennepohl and E. I. Solomon, *Chem. Rev.*, 1996, **96**, 2239–2314.
3 Selected reviews: (*a*) A. C. Ghosh, C. Duboc and M. Gennari, *Coord. Chem. Rev.*, 2021, **428**, 213606; (*b*) C.-H. Wang and S. DeBeer, *Chem. Soc. Rev.*, 2021, **50**, 8743–8761; (*c*) C. Ferousi, S. H. Majer, I. M. DiMucci and K. M. Lancaster, *Chem. Rev.*, 2020, **120**, 5252–5307; (*d*) J. Serrano-Plana, I. Garcia-Bosch, A. Company and M. Costas, *Acc. Chem. Res.*, 2015, **48**, 2397–2406; (*e*) M. D. Kärkäs, O. Verho, E. V. Johnston and B. Åkermark, *Chem. Rev.*, 2014, **114**, 11863–12001; (*f*) M. Costas, K. Chen and L. Que Jr, *Coord. Chem. Rev.*, 2000, **200–202**, 517–544.
4 (*a*) C. Uyeda and C. M. Farley, *Acc. Chem. Res.*, 2021, **54**, 3710–3719; (*b*) I. G. Powers and C. Uyeda, *ACS Catal.*, 2017, **7**, 936–958; (*c*) D. C. Powers and T. Ritter, *Acc. Chem. Res.*, 2012, **45**, 840–850.
5 J. Bauer, H. Braunschweig and R. D. Dewhurst, *Chem. Rev.*, 2012, **112**, 4329–4346.
6 (*a*) R. Govindarajan, S. Deolka and J. R. Khusnutdinova, *Chem. Sci.*, 2022, **13**, 14008–14031; (*b*) N. P. Mankad, *Chem. Commun.*, 2018, **54**, 1291–1302; (*c*) L. H. Gade, *Angew. Chem., Int. Ed.*, 2000, **39**, 2658–2678.
7 (*a*) H.-C. Yu, S. M. Islam and N. P. Mankad, *ACS Catal.*, 2020, **10**, 3670–3675; (*b*) L.-J. Cheng and N. P. Mankad, *J. Am. Chem. Soc.*, 2019, **141**, 3710–3716; (*c*) M. K. Karunananda and N. P. Mankad, *J. Am. Chem. Soc.*, 2015, **137**, 14598–14601; (*d*) S. R. Parmelee, T. J. Mazzacano, Y. Zhu, N. P. Mankad

Open Access Article. Published on 07 December 2023. Downloaded on 2/7/2026 10:15:02 PM. This article is licensed under a Creative Commons Attribution-NonCommercial 3.0 Unported Licence.

and J. A. Keith, *ACS Catal.*, 2015, **5**, 3689–3699; (*e*) T. J. Mazzacano and N. P. Mankad, *J. Am. Chem. Soc.*, 2013, **135**, 17258–17261.

8 (*a*) M. Navarro, J. J. Moreno, M. Pérez-Jiménez and J. Campos, *Chem. Commun.*, 2022, **58**, 11220–11235; (*b*) B. Chatterjee, W.-C. Chang, S. Jena and C. Werlé, *ACS Catal.*, 2020, **10**, 14024–14055.

9 (*a*) N. Hidalgo, F. de la Cruz-Martínez, M. T. Martín, M. C. Nicasio and J. Campos, *Chem. Commun.*, 2022, **58**, 9144–9147; (*b*) N. Hidalgo, J. J. Moreno, M. Pérez-Jiménez, C. Maya, J. López-Serrano and J. Campos, *Chem.–Eur. J.*, 2020, **26**, 5982–5993; (*c*) J. Campos, *J. Am. Chem. Soc.*, 2017, **139**, 2944–2947.

10 E. S. Osipova, E. S. Gulyaeva, E. I. Gutsul, V. A. Kirkina, A. A. Pavlov, Y. V. Nelyubina, A. Rossin, M. Peruzzini, L. M. Epstein, N. V. Belkova, O. A. Filippov and E. S. Shubina, *Chem. Sci.*, 2021, **12**, 3682–3692.

11 E. S. Osipova, D. V. Sedlova, E. I. Gutsul, Yu. V. Nelyubina, P. V. Dorovatovskii, L. M. Epstein, O. A. Filippov, E. S. Shubina and N. V. Belkova, *Organometallics*, 2023, **42**, 2651–2660.

12 S. Sinhababu, M. R. Radzhabov, J. Telser and N. P. Mankad, *J. Am. Chem. Soc.*, 2022, **144**, 3210–3221.

13 E. S. Osipova, E. S. Gulyaeva, N. V. Kireev, S. A. Kovalenko, C. Bijani, Y. Canac, D. A. Valyaev, O. A. Filippov, N. V. Belkova and E. S. Shubina, *Chem. Commun.*, 2022, **58**, 5017–5020.

14 E. S. Osipova, S. A. Kovalenko, E. S. Gulyaeva, N. V. Kireev, A. A. Pavlov, O. A. Filippov, A. A. Danshina, D. A. Valyaev, Y. Canac, E. S. Shubina and N. V. Belkova, *Molecules*, 2023, **28**, 3368.

15 (*a*) H. R. Sharpe, A. M. Geer, T. J. Blundell, F. R. Hastings, M. W. Fay, G. A. Rance, W. Lewis, A. J. Blake and D. L. Kays, *Catal. Sci. Technol.*, 2017, **8**, 229–235; (*b*) S. Muhammad, S. Moncho, E. N. Brothers and A. A. Bengali, *Chem. Commun.*, 2014, **50**, 5874–5877; (*c*) T. Kakizawa, Y. Kawano, K. Naganeyama and M. Shimoi, *Chem. Lett.*, 2011, **40**, 171–173.

16 Previously described synthesis of $\mathbf{3^{Br}}$ (ref.16) was reoptimized using weak base (K_2CO_3) in DMF at 120 °C to give target product in 82% yield avoiding the generation of free bis(NHC) with strong bases(*a*) Y. Yang, Z. Zhang, X. Chang, Y.-Q. Zhang, R.-Z. Liao and L. Duan, *Inorg. Chem.*, 2020, **59**, 10234–10242; (*b*) M. Pinto, S. Friães, F. Franco, J. Lloret-Fillol and B. Royo, *ChemCatChem*, 2018, **10**, 2734–2740.

17 W.-W. Zhan, Q.-L. Zhu and Q. Xu, *ACS Catal.*, 2016, **6**, 6892–6905.

18 For the formation of Mn/Hg intermetallic compounds, see: (*a*) Z. Moser and C. Guminski, *J. Phase Equilib.*, 1993, **14**, 726–733; (*b*) J. F. de Wet, *Angew. Chem.*, 1955, **67**, 208; (*c*) O. Prelinger, *Monatsh. Chem.*, 1893, **14**, 353–370.

19 (*a*) E. A. LaPierre, B. O. Patrick and I. Manners, *J. Am. Chem. Soc.*, 2019, **141**, 20009–20015; (*b*) C. Lichtenberg, L. Viciu, M. Adelhardt, J. Sutter, K. Meyer, B. de Bruin and H. Grützmacher, *Angew. Chem., Int. Ed.*, 2015, **54**, 5766–5771; (*c*) J. R. Vance, A. Schäfer, A. P. M. Robertson, K. Lee, J. Turner, G. R. Whittell and I. Manners, *J. Am. Chem. Soc.*, 2014, **136**, 3048–3064; (*d*) T.-P. Lin and J. C. Peters, *J. Am. Chem. Soc.*, 2013, **135**, 15310–15313; (*e*) M. Vogt, B. de Bruin, H. Berke, M. Trincado and H. Grützmacher, *Chem. Sci.*, 2011, **2**, 723–727; (*f*) M. E. Sloan, A. Staubitz, T. J. Clark, C. A. Russell, G. C. Lloyd-Jones and I. Manners, *J. Am. Chem. Soc.*, 2010, **132**, 3831–3841; (*g*) Y. Kawano, M. Uruichi, M. Shimoi, S. Taki, T. Kawaguchi, T. Kakizawa and H. Ogino, *J. Am. Chem. Soc.*, 2009, **131**, 14946–14957.

20 For noble metal catalysts for DMAB dehydrogenation working at 0.5 mol% charge or below, see: (*a*) S. Pal, S. Kusumoto and K. Nozaki, *Organometallics*, 2018, **37**, 906–914; (*b*) E. H. Kwan, H. Ogawa and M. A. Yamashita, *ChemCatChem*, 2017, **9**, 2457–2462; (*c*) E. U. Barın, M. Masjedi and S. Özkar, *Materials*, 2015, **8**, 3155–3167; (*d*) H. C. Johnson, E. M. Leitao, G. R. Whittell, I. Manners, G. C. Lloyd-Jones and A. S. Weller, *J. Am. Chem. Soc.*, 2014, **136**, 9078–9093; (*e*) D. F. Schreiber, C. O'Connor, C. Grave, Y. Ortin, H. Müller-Bunz and A. D. Phillips, *ACS Catal.*, 2012, **2**, 2505–2511; (*f*) R. Dallanegra, A. P. M. Robertson, A. B. Chaplin, I. Manners and A. S. Weller, *Chem. Commun.*, 2011, **47**, 3763–3765; (*g*) A. Friedrich, M. Drees and S. Schneider, *Chem.–Eur. J.*, 2009, **15**, 10339–10342.

21 For reviews on amine-boranes dehydrogenation using catalysts based on main-group elements, see: (*a*) D. H. A. Boom, A. R. Jupp and J. C. Slootweg, *Chem.–Eur. J.*, 2019, **25**, 9133–9152; (*b*) R. L. Melen, *Chem. Soc. Rev.*, 2016, **45**, 775–788.

22 Alkaline metal catalysts: (*a*) R. McLellan, A. R. Kennedy, R. E. Mulvey, S. A. Orr and S. D. Robertson, *Chem.–Eur. J.*, 2017, **23**, 16853–16861; (*b*) P. Bellham, M. S. Hill and G. Kociok-Köhn, *Dalton Trans.*, 2015, **44**, 12078–12081.

23 Alkaline earth metal catalysts: (*a*) L. Wirtz, K. Y. Ghulam, B. Morgenstern and A. Schäfer, *ChemCatChem*, 2022, **14**, e202201007; (*b*) L. Wirtz, W. Haider, V. Huch, M. Zimmer and A. Schäfer, *Chem.–Eur. J.*, 2020, **26**, 6176–6184; (*c*) A. C. A. Ried, L. J. Taylor, A. M. Geer, H. E. L. Williams, W. Lewis, A. J. Blake and D. L. Kays, *Chem.–Eur. J.*, 2019, **25**, 6840–6846; (*d*) X. Zheng, J. Huang, Y. Yao and X. Xu, *Chem. Commun.*, 2019, **55**, 9152–9155; (*e*) D. J. Liptrot, M. S. Hill, M. F. Mahon and D. J. MacDougall, *Chem.–Eur. J.*, 2010, **16**, 8508–8515.

24 Group 3 metal catalysts: (*a*) P. Xu and X. Xu, *Organometallics*, 2019, **38**, 3212–3217; (*b*) E. Lu, Y. Yuan, Y. Chen and W. Xia, *ACS Catal.*, 2013, **3**, 521–524; (*c*) H. J. Cowley, M. S. Holt, R. L. Melen, J. M. Rawson and D. S. Wright, *Chem. Commun.*, 2011, **47**, 2682–2684; (*d*) M. S. Hill, G. Kociok-Köhn and T. P. Robinson, *Chem. Commun.*, 2010, **46**, 7587–7589.

25 Lanthanide- and actinide-based catalysts: (*a*) V. A. Kirkina, A. A. Kissel, A. N. Selikhov, Y. V. Nelyubina, O. A. Filippov, N. V. Belkova, A. A. Trifonov and E. S. Shubina, *Chem. Commun.*, 2022, **58**, 859–862; (*b*) K. A. Erickson and J. L. Kiplinger, *ACS Catal.*, 2017, **7**, 4276–4280; (*c*) P. Cui, T. P. Spaniol, L. Maron and J. Okuda, *Chem.–Eur. J.*, 2013, **19**, 13437–13444.

© 2024 The Author(s). Published by the Royal Society of Chemistry

Open Access Article. Published on 07 December 2023. Downloaded on 2/7/2026 10:15:02 PM. This article is licensed under a Creative Commons Attribution-NonCommercial 3.0 Unported Licence.

26 (*a*) M. Boudjelel, E. D. Sosa Carrizo, S. Mallet-Ladeira, S. Massou, K. Miqueu, G. Bouhadir and D. Bourissou, *ACS Catal.*, 2018, **8**, 4459–4464; (*b*) C. Appelt, J. C. Slootweg, K. Lammertsma and W. Uhl, *Angew. Chem., Int. Ed.*, 2013, **52**, 4256–4259; (*c*) A. M. Chapman, M. F. Haddow and D. F. Wass, *J. Am. Chem. Soc.*, 2011, **133**, 8826–8829.

27 S. Duman, M. Masjedi and S. Özkar, *J. Mol. Catal. A: Chem.*, 2016, **411**, 9–18.

28 (*a*) A. Staubitz, A. P. M. Robertson and I. Manners, *Chem. Rev.*, 2010, **110**, 4079–4124; (*b*) C. W. Hamilton, R. T. Baker, A. Staubitz and I. Manners, *Chem. Soc. Rev.*, 2009, **38**, 279–293.

29 (*a*) K. A. Erickson, J. P. W. Stelmach, N. T. Mucha and R. Waterman, *Organometallics*, 2015, **34**, 4693–4699; (*b*) D. García-Vivó, E. Huergo, M. A. Ruiz and R. Travieso-Puente, *Eur. J. Inorg. Chem.*, 2013, **2013**, 4998–5008.

30 (*a*) F. Anke, S. Boye, A. Spannenberg, A. Lederer, D. Heller and T. Beweries, *Chem.–Eur. J.*, 2020, **26**, 7889–7899; (*b*) T. M. Maier, S. Sandl, I. G. Shenderovich, A. J. von Wangelin, J. J. Weigand and R. Wolf, *Chem.–Eur. J.*, 2019, **25**, 238–245; (*c*) T. Jurca, T. Dellermann, N. E. Stubbs, D. A. Resendiz-Lara, G. R. Whittell and I. Manners, *Chem. Sci.*, 2018, **9**, 3360–3366; (*d*) F. Anke, D. Han, M. Klahn, A. Spannenberg and T. Beweries, *Dalton Trans.*, 2017, **46**, 6843–6847; (*e*) C. Lichtenberg, M. Adelhardt, T. L. Gianetti, K. Meyer, B. de Bruin and H. Grützmacher, *ACS Catal.*, 2015, **5**, 6230–6240.

31 T. M. Boyd, K. A. Andrea, K. Baston, A. Johnson, D. E. Ryan and A. S. Weller, *Chem. Commun.*, 2020, **56**, 482–485.

32 (*a*) P. Bhattacharya, J. A. Krause and H. Guan, *J. Am. Chem. Soc.*, 2014, **136**, 11153–11161; (*b*) R. T. Baker, J. C. Gordon, C. W. Hamilton, N. J. Henson, P.-H. Lin, S. Maguire, M. Murugesu, B. L. Scott and N. C. Smythe, *J. Am. Chem. Soc.*, 2012, **134**, 5598–5609; (*c*) R. J. Keaton, J. M. Blacquiere and R. T. Baker, *J. Am. Chem. Soc.*, 2007, **129**, 1844–1845.

33 (*a*) M. Hasenbeck, J. Becker and U. Gellrich, *Angew. Chem., Int. Ed.*, 2020, **59**, 1590–1594; (*b*) Z. Mo, A. Rit, J. Campos, E. L. Kolychev and S. Aldridge, *J. Am. Chem. Soc.*, 2016, **138**, 3306–3309; (*c*) Z. Lu, L. Schweighauser, H. Hausmann and H. A. Wegner, *Angew. Chem., Int. Ed.*, 2015, **54**, 15556–15559; (*d*) W. C. Ewing, A. Marchione, D. W. Himmelberger, P. J. Carroll and L. G. Sneddon, *J. Am. Chem. Soc.*, 2011, **133**, 17093–17099.

34 (*a*) K. Sarkar, K. Das, A. Kundu, D. Adhikari and B. Maji, *ACS Catal.*, 2021, **11**, 2786–2794; (*b*) M. Gediga, C. M. Feil, S. H. Schlindwein, J. Bender, M. Nieger and D. Gudat, *Chem.–Eur. J.*, 2017, **23**, 11560–11569.

35 (*a*) D. Wei, X. Shi, P. Sponholz, H. Junge and M. Beller, *ACS Cent. Sci.*, 2022, **8**, 1457–1463; (*b*) D. Wei, R. Sang, P. Sponholz, H. Junge and M. Beller, *Nat. Energy*, 2022, **7**, 438–447; (*c*) A. Léval, A. Agapova, C. Steinlechner, E. Alberico, H. Junge and M. Beller, *Green Chem.*, 2020, **22**, 913–920.

36 (*a*) A. Rossin and M. Peruzzini, *Chem. Rev.*, 2016, **116**, 8848–8872; (*b*) S. Bhunya, T. Malakar, G. Ganguly and A. Paul, *ACS Catal.*, 2016, **6**, 7907–7934.

37 N. V. Kireev, O. A. Filippov, E. S. Gulyaeva, E. S. Shubina, L. Vendier, Y. Canac, J.-B. Sortais, N. Lugan and D. A. Valyaev, *Chem. Commun.*, 2020, **56**, 2139–2142.

38 R. Buhaibeh, O. A. Filippov, A. Bruneau-Voisine, J. Willot, C. Duhayon, D. A. Valyaev, N. Lugan, Y. Canac and J.-B. Sortais, *Angew. Chem., Int. Ed.*, 2019, **58**, 6727–6731.

39 (*a*) S. C. A. Sousa, S. Realista and B. Royo, *Adv. Synth. Catal.*, 2020, **362**, 2437–2443; (*b*) B. Royo, C. J. Carrasco, S. C. A. Sousa and M. F. Pinto, *ChemCatChem*, 2019, **11**, 3839–3843.

40 (*a*) S. Fernández, F. Franco, M. Martínez Belmonte, S. Friães, B. Royo, J. M. Luis and J. Lloret-Fillol, *ACS Catal.*, 2023, **13**, 10375–10385; (*b*) F. Franco, F. P. Mara, B. Royo and J. Lloret-Fillol, *Angew. Chem., Int. Ed.*, 2018, **57**, 4603–4606.

41 (*a*) N. F. Both, A. Spannenberg, H. Jiao, K. Junge and M. Beller, *Angew. Chem., Int. Ed.*, 2023, **62**, e202307987; (*b*) K. Azouzi, L. Pedussaut, R. Pointis, A. Bonfiglio, R. Kumari Riddhi, C. Duhayon, S. Bastin and J.-B. Sortais, *Organometallics*, 2023, **42**, 1832–1838.

42 (*a*) K. Ganguli, A. Mandal and S. Kundu, *ACS Catal.*, 2022, **12**, 12444–12457; (*b*) X.-B. Lan, Z. Ye, J. Liu, M. Huang, Y. Shao, X. Cai, Y. Liu and Z. Ke, *ChemSusChem*, 2020, **13**, 2557–2563; (*c*) X.-B. Lan, Z. Ye, M. Huang, J. Liu, Y. Liu and Z. Ke, *Org. Lett.*, 2019, **21**, 8065–8070; (*d*) M. Huang, Y. Li, Y. Li, J. Liu, S. Shu, Y. Liu and Z. Ke, *Chem. Commun.*, 2019, **55**, 6213–6216.

43 (*a*) K. Lindenau, N. Jannsen, M. Rippke, H. Al Hamwi, C. Selle, H.-J. Drexler, A. Spannenberg, M. Sawall, K. Neymeyr, D. Heller, F. Reiß and T. Beweries, *Catal. Sci. Technol.*, 2021, **11**, 4034–4050; (*b*) C. Cesari, B. Berti, F. Calcagno, C. Lucarelli, M. Garavelli, R. Mazzoni, I. Rivalta and S. Zacchini, *Organometallics*, 2021, **40**, 2724–2735; (*c*) M. Trose, M. Reiß, F. Reiß, F. Anke, A. Spannenberg, S. Boye, A. Lederer, P. Arndt and T. Beweries, *Dalton Trans.*, 2018, **47**, 12858–12862; (*d*) T. Miyazaki, Y. Tanabe, M. Yuki, Y. Miyake and Y. Nishibayashi, *Organometallics*, 2011, **30**, 2394–2404.

44 (*a*) T. Yasue, Y. Kawano and M. Shimoi, *Angew. Chem., Int. Ed.*, 2003, **42**, 1727–1730; (*b*) T. Kakizawa, Y. Kawano and M. Shimoi, *Organometallics*, 2001, **20**, 3211–3213.

45 (*a*) N. V. Belkova, L. M. Epstein, O. A. Filippov and E. S. Shubina, *Chem. Rev.*, 2016, **116**, 8545–8587; (*b*) N. V. Belkova, L. M. Epstein and E. S. Shubina, *Eur. J. Inorg. Chem.*, 2010, **2010**, 3555–3565.

© 2024 The Author(s). Published by the Royal Society of Chemistry